International Journal of Mass Spectrometry 280 (2009) 85–92

Contents lists available at ScienceDirect

International Journal of Mass Spectrometry

journal homepage: www.elsevier.com/locate/ijms

Electron-transfer and chemical reactivity following collisions of Ar^{2+} with C_2H_2

Michael A. Parkes*, Jessica F. Lockyear, Stephen D. Price*

Department of Chemistry, University College London, 20 Gordon Street, London WC1H 0AJ, United Kingdom

ARTICLE INFO

Article history:
Received 29 May 2008
Received in revised form 18 July 2008
Accepted 23 July 2008
Available online 3 August 2008

Dedicated to Zdenek Herman on the occasion of his 75th birthday.

Keywords:
Ionisation
Ion-molecule
Dication
Ethyne
Coincidence

ABSTRACT

The reaction between Ar^{2+} and C_2H_2 has been studied, at centre-of-mass collision energies ranging from 3 to 7 eV, using a position-sensitive coincidence technique to detect the monocation pairs, which are formed. Sixteen different reaction channels generating pairs of monocations have been observed, these channels arise from double-electron-transfer, single-electron-transfer and chemical reactions forming ArC^+. Examination of the scattering diagrams and energetic information extracted from the coincidence data indicate that double-electron-transfer is a direct process, which does not involve a collision complex, and the derived energetics point towards a concerted, not stepwise, mechanism for the two-electron-transfer. As is commonly observed, single-electron-transfer from C_2H_2 to Ar^{2+} takes place *via* a direct mechanism, again not involving complexation. Most of the $C_2H_2^+$ products that are formed in the single-electron-transfer reactions possess significant (12–15 eV) internal energy and fragment rapidly within the electric field of the partner Ar^+ ion. The chemical reactions appear to proceed *via* a direct mechanism involving the initial formation of $ArCH^+$, which subsequently fragments to form ArC^+.

1. Introduction

As discussed in recent reviews [1,2], ethyne (C_2H_2) is the smallest stable hydrocarbon, which contains a carbon–carbon bond and has been studied in depth by many advanced theoretical and experimental techniques. Ethyne also has many technological uses, for example in arc-welding and as a fuel for flames [3]. In addition, plasmas composed of Ar and C_2H_2 are used for the surface deposition of diamond films [4–6]. Ethyne is also an important component of many planetary atmospheres [7], especially that of Titan [8], and is also found in the Earth's atmosphere [1]. All the above are environments where the formation of ions may be important, and it is therefore of fundamental interest to understand the ionisation of C_2H_2 and its consequences.

There are a considerable number of studies of the single and double ionisation of ethyne reported in the literature. Single ionisation of ethyne has been extensively investigated using photon ionisation [9–12], photoelectron spectroscopy ([13–15] and references therein) as well as coincidence techniques [16–20], and the electron ionisation of ethyne has recently been reviewed [21]. Double ionisation of ethyne has been studied *via* photon ionisation [22–24], electron ionisation [21], charge stripping [25–27] and Auger spectroscopy [28–30]. Far less attention has been paid to the reactions of ethyne with dications, or the reactions of doubly ionised ethyne itself. Roithová and Schröder have studied the reactions of various aromatic organic dications with neutral ethyne [31]. These experiments observed charge-conserving bond-forming processes, in addition to the expected electron-transfer, proton transfer, and collision-induced dissociation reactions; for example $C_7H_6^{2+}$ and C_2H_2 react to give $C_9H_7^{2+}$. Böhme and co-workers have studied the reactions of C_{60}^{x+} and C_{70}^{x+} (where $x = 1–3$) with C_2H_2 in a selected ion flow tube and found there was no simple bimolecular reaction, only three-body adduct formation [32]. Reactions of Ar^{2+} with C_2H_2 have been studied using an ion drift tube [33,34] and $C_2H_2^+$ and C_2H^+ were detected as products. These drift tube experiments indicated the reaction rate coefficient was large and remained constant over a range of collision energies below 1 eV.

This study will consider three of the general classes of reactivity [35–43] which can occur following collisions between a dication M^{2+} and a neutral species AB: double-electron-transfer (DET), single-electron-transfer (SET) and chemical reactions. In DET two electrons are transferred to M^{2+}, from the neutral, to generate AB^{2+}; hence, any monocationic products detected will be due to the dissociation of AB^{2+}. In SET one electron is transferred to M^{2+} from AB yielding M^+ and AB^+ as the primary products. Both the DET and SET mechanisms can be further categorized as *dissociative* or *non-dissociative*. If the reaction is non-dissociative then the ionic products from the primary electron-transfer are formed in stable electronic states. Conversely, if the reaction is dissociative one or both of the primary ionic products subsequently fragment

* Corresponding authors. Tel.: +44 20 7679 4606; fax: +44 20 7679 7463.
E-mail addresses: michael.parkes@ucl.ac.uk (M.A. Parkes), s.d.price@ucl.ac.uk (S.D. Price).

1387-3806/$ – see front matter © 2008 Elsevier B.V. All rights reserved.
doi:10.1016/j.ijms.2008.07.027

further. As the position-sensitive coincidence (PSCO) method we employ detects only pairs of monocations, only dissociative DET will be detected by our experiments, even if there are non-dissociative channels operating. However, both dissociative and non-dissociative SET events can be probed by the PSCO methodology. In a "chemical" process new bonds are generated between atoms from the reactant dication and atoms from the neutral reactant. Again, chemical processes forming pairs of ions can be probed by the PSCO technique, but reactions, which generate dicationic products, will not be detected.

At low collision energies, below 100 eV, SET reactions of dications can be well explained using 'reaction window' models based on the Landau–Zener theory [40,44,45]. Briefly, for a dication reaction, this model pictures the electron-transfer occurring at a curve crossing (Fig. 1(b)) between a reactant potential energy curve ($M^{2+} + AB$), which is attractive at significant interspecies separations, and a product potential ($M^{+} + AB^{+}$), which is dominated by Coulomb repulsion. The one-dimensional Landau–Zener model indicates that, for efficient SET, this crossing of potential energy curves (PECs) should occur at interspecies separations between 3 and 6 Å. If the curve crossing is at larger interspecies separations than the favoured window, the coupling between the reactant and product potentials is not strong enough for efficient electron-transfer. Conversely, if the curve crossing is at too small an interspecies separation the coupling between the reactant and product potentials is strong. However, this strong interaction results in inefficient net electron-transfer, as the collision system has to pass through the curve crossing twice, on approach and separation.

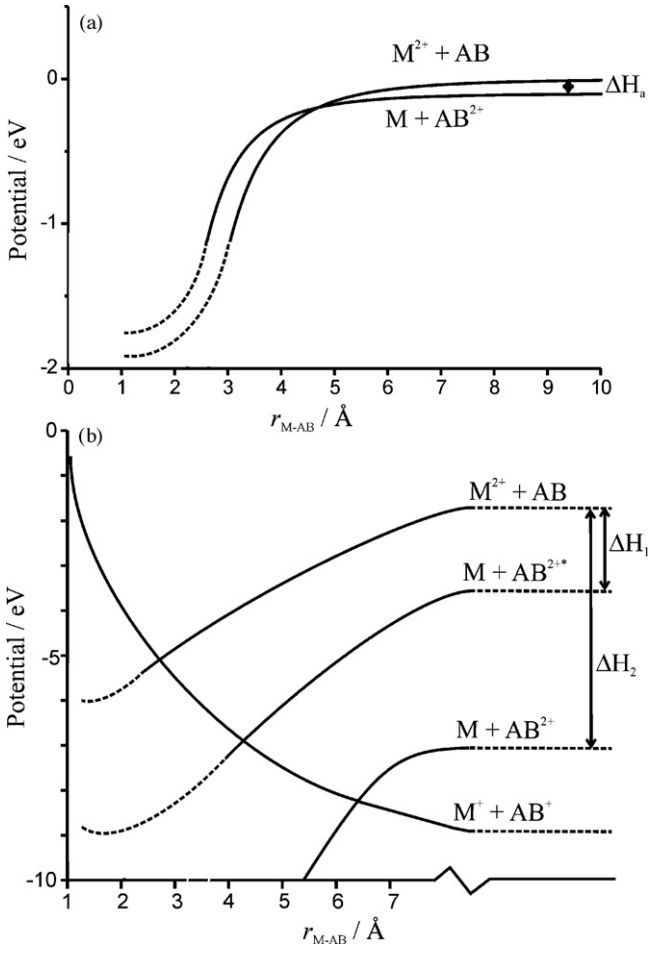

Fig. 1. Schematic potential energy curves for (a) concerted and (b) sequential double-electron-transfer following the reaction of M^{2+} with AB. (a) ΔH_a indicates the small reaction enthalpy which is required for the curve crossing to lie in the reaction window for the concerted mechanism. (b) The competition between single- and double-electron-transfer, which is implicit if the sequential mechanism for double-electron-transfer is operating. The sequential mechanism involves an initial single-electron-transfer to the repulsive potential corresponding to a pair of monocations. The system may then remain on this potential, resulting in single-electron-transfer, or cross again to reach an $M + AB^{2+}$ asymptote. ΔH_1 and ΔH_2 schematically indicate the limiting reaction exothermicities for which this pair of curve crossings will lie in the reaction window, a markedly larger range of exothermicities than for the concerted mechanism illustrated in (a).

For the DET reactions of dications with neutrals, the simple one-dimensional reactant and product potentials will have similar forms at larger interspecies separations, as both are dominated by dication-neutral polarisation attraction. At low collision energies, symmetric DET processes have been investigated for atomic species (e.g., $Ne^{2+} + Ne$) and the measured cross-sections agree reasonably well with simple models [46–50]. DET in non-symmetric collision systems involving dications, at low collision energies, has been observed before [44,51,52] but not, to our knowledge, investigated in any great detail. Within the constraints of the one-dimensional Landau–Zener model, non-resonant DET in low-energy collisions between the generic chemical species M^{2+} and AB can, in principle, occur by two routes. The first pathway is that the two electrons are both transferred at the crossing of the $M^{2+} + AB$ and the $M + AB^{2+}$ PECs, Fig. 1(a), a concerted process. Under a one-dimensional simple electrostatic model, the only differences in the forms of the reactant and product PECs, beyond the repulsive short-range interactions, are due to the differing polarisabilities of the respective neutral species. Thus, the concerted DET pathway requires the reactant and product asymptotes to lie close in energy, within 1 eV, to place the curve crossing in the reaction window (Fig. 1(a)). An alternative DET pathway, which has been proposed before [44], involves sequential electron-transfer *via* a repulsive $M^{+} + AB^{+}$ potential which links the attractive reactant and product potentials, as illustrated in Fig. 1(b). The reactive system first crosses from the $M^{2+} + AB$ potential to the $M^{+} + AB^{+}$ potential, followed by a second crossing to the $M + AB^{2+}$ surface. Interestingly, this sequential mechanism implies an intrinsic competition between DET and SET. Qualitatively, the relevant curve crossings in this sequential model of DET will lie in the reaction window for a much wider range of reaction exothermicities than for the concerted mechanism. Thus, if the sequential DET mechanism was favoured we would expect that DET should be a common outcome of dication-neutral collisions. The relative scarcity of dication DET reactions following dication-neutral collisions, at low collision energies, perhaps hints that the concerted, "near-resonant", mechanism is the effective pathway for these processes [52].

This paper reports an investigation of the reactivity of Ar^{2+} with neutral C_2H_2, at collision energies from 3 to 7 eV in the centre-of-mass (CM) frame using a time-of-flight mass spectrometer, equipped with a position-sensitive detector (PSD). This apparatus allows the coincident detection of the monocation pairs formed following the reactive encounters. As well as identification of the monocation pairs, this PSCO technique allows the determination of the velocity vectors of the reaction products giving a unique insight into the dynamics of the dication reactions.

2. Experimental

The PSCO apparatus has been described in detail before in the literature [35,53–55]. Briefly, dications, and other ions, are generated from a suitable precursor gas by electron ionisation in a custom-built ion source. The cations are then extracted from the ion source and transmitted into a hemispherical energy-analyser where they are energy-selected to give an ion beam with an energy

spread of approximately 0.3 eV. At the exit of the analyser, the ion beam is pulsed by a pair of deflectors which sweep the beam backwards and forwards across a small aperture. The pulses of ions then pass through a series of ion optics, which accelerate and focus the beam, before it enters a commercial velocity filter which is set to transmit the dication of interest [56]. The resulting mass-selected pulses of ions are then decelerated before entering the interaction region, which doubles as the source region of a time-of-flight mass spectrometer (TOFMS).

In the interaction region the pulses of dications cross an effusive jet of neutral gas. The pressure of the neutral species is low enough so that any reactions take place under single-collision conditions. The interaction region is initially maintained in a field-free state, so that any reactions take place at the intended low collision energy. Once a dication pulse has reached the centre of the interaction region, a voltage is applied to a repeller plate, which drives the ions into the acceleration region of the TOFMS. Generally the repeller voltage is pulsed to +300 V to allow the collection of all the product ions, at the expense of some energy resolution. If increased energy resolution is required, a lower repeller voltage (50 V) can be used, but under these conditions ions with significant off-axis velocity components will then miss the detector, limiting the range of the angular scattering observed.

Approximately 0.5 μs after the repeller pulse, a start pulse is sent to a time to digital converter, which receives stop signals from the PSD at the end of the TOFMS. The PSD is a commercial wire-round delay line anode (RoentDek DLD 80) which gives the ion's time-of-flight and the position (x, y) of the ionic impact on the face of the PSD. When two ion signals are detected following a repeller plate pulse they are recorded as a coincidence, and the positional and timing information stored. If only a single ion is detected in a pulse then its TOF is added to a simple TOF mass spectrum. To ensure that true coincidences are dominant, the experimental event rate is kept low, so that on average far less than one ion per repeller plate pulse is detected. This reduces the false coincidence rate to such an extent that there is rarely a need to deal with such signals in the PSCO spectrum.

As has been shown before [53], from the positional and timing information for each pair of product ions detected it is possible to calculate the x, y and z velocity vectors for each ion in the laboratory frame. The details of this data treatment have been presented previously and will not be repeated in detail here [35,53–55,57–59]. Briefly, the x and y velocities are derived from the position of the ionic impacts at the detector, whilst the z (on-axis) velocity can be determined from the deviation of the measured ionic TOF from the TOF the ion would have if it possessed zero initial kinetic energy. These laboratory frame velocities are then converted to velocities in the CM frame $w(X^+)$ for ease of interpretation. This conversion is done using the velocity of the CM in the laboratory frame, which can be determined from the initial dication velocity or the mutual velocities of the products of a reactive channel that produces only a pair of monocations [53].

As well as generating just pairs of monocations (*two-body* reactions), the reactions of dications with molecules will often generate a neutral species in addition to the pair of monocations, exhibiting so-called *three-body* reactivity. Using conservation of momentum in the CM frame, the CM velocity of the neutral species formed in such a three-body reaction can be determined from the velocities of the ionic species derived from the PSCO data. When all the product velocities have been determined, the correlations between these vectors can be explored for the different reactive channels, such correlations have proven to be a powerful probe of the reaction mechanism [35]. Of course, if a given reactive channel generates more than a single neutral species, in addition to the pair of monocations, conservation of momentum cannot be used to derive the neutrals' respective velocities. The correlations between the product velocities are normally displayed *via* two classes of scattering diagram. Scattering diagrams in the CM frame are polar histograms where, for a product ion X^+, $|w(X^+)|$ is plotted as the radial co-ordinate and the scattering angle θ ($0^\circ \le \theta \le 180^\circ$) between the product's velocity vector and the reactant dication's velocity $w(M^{2+})$ is the angular co-ordinate. Typically, the data for one product is displayed in the upper semi-circle of the diagram and the data for a second product is plotted in the lower semi-circle. Internal-frame scattering diagrams are also a powerful method of inspecting the coincidence data [35]. Here, the scattering of a product (e.g., X^+) is displayed with reference to the velocity vector of another product (Y), $w(Y)$. Again, $|w(X^+)|$ is the radial co-ordinate and the angular co-ordinate is the angle ϕ ($0^\circ \le \phi \le 180^\circ$) between $w(X^+)$ and $w(Y)$. In such internal-frame scattering diagrams the scattering data for the second product, again with respect to the reference species Y, can be displayed in the lower half of the diagram.

In addition to scattering diagrams, the PSCO experiment provides energetic information on the different reactive channels that are detected. Initially, the kinetic energy release T can be derived from the product velocities in the CM frame for a given reactive channel. Then the translational exothermicity (ΔE_T) for each reactive event can be expressed in terms of T and the CM collision energy of the reactive system E_{cm}:

$$\Delta E_T = E_{products} - E_{reactants} = T - E_{cm} \quad (1)$$

where the energies of the products and reactants, $E_{products}$ and $E_{reactants}$, can contain contributions from rotational, vibrational and electronic excitation. If there is no internal excitation of the products or the reactants then ΔE_T is simply the enthalpy of reaction, $\Delta_r H$. As both T and E_{cm} can be determined for each reactive event detected during the experiment it is possible to produce a histogram of the ΔE_T for each reactive channel, which we refer to as a translational exothermicity spectrum (TES). This spectrum can provide information on the energies of the electronic, and in an ideal case the vibrational, states involved [53–55,60]. As discussed below, for the channels where more than one neutral species may be formed, it is sometimes possible to use the TES to deduce the identity of the neutral product(s).

Previous studies of the reactions of Ar^{2+}, using both the PSCO apparatus and employing other experimental techniques, have shown that the reactant dication beam comprises ions in the three electronic states arising from the $3p^{-2}$ configuration, namely the $^3P_{2,1,0}$ $^1D_2$ and $^1S_0$ states [54,61,62]. The latter levels lying 1.7 and 4.1 eV above the ground state, respectively [63]. These earlier investigations indicate these Ar^{2+} states should be present in their statistical ratio of 9:5:1.

3. Results and discussion

PSCO spectra were recorded following collisions of Ar^{2+} with C_2H_2 at five different CM collision energies ranging between 3 and 7 eV. Nine different ionic products were detected in the mass spectrum, Ar^+, $C_2H_2^+$, C_2H^+, C_2^+, CH_2^+, CH^+, C^+, H^+ and ArC^+. Of course, it is also possible that long-lived $C_2H_2^{2+}$ ions are also formed. However, due to the presence of the strong signals due to CH^+ product ions, any long-lived isobaric $C_2H_2^{2+}$ ions could not be definitively identified. The coincidence spectrum revealed sixteen different reaction channels involving the production of ion pairs, the different channels and their relative branching ratios are listed in Table 1. Since all sixteen reactive channels are monitored in the same PSCO experiment, the branching ratios are readily derived from the coincidence counts for each channel in the PSCO pairs spectrum [35].

Table 1
Observed channels and their branching ratios following the reaction of Ar^{2+} with C_2H_2

Number reaction	$\Delta_r H^\circ$ (eV)	Branching ratio
Double-electron-transfer		
$C^+ + H^+ + CH + Ar$ (1)	−5.04	0.01
$CH^+ + H^+ + C + Ar$ (2)	−5.64	0.03
$CH^+ + C^+ + H + Ar$ (3)	−7.98	0.07
$CH^+ + CH^+ + Ar$ (4)	−12.11	0.03
$C_2^+ + H^+ + H + Ar$ (5)	−7.54	0.03
$C_2H^+ + H^+ + Ar$ (6)	−13.33	0.002
Single-electron-transfer		
$Ar^+ + H^+ + C_2H$ (7)	−14.12	0.03
$Ar^+ + C^+ + CH_2$ (8)	−7.29	0.03
$Ar^+ + CH^+ + CH$ (9)	−7.01	0.22
$Ar^+ + CH_2^+ + C$ (10)	−8.19	0.03
$Ar^+ + C_2^+ + H_2$ (11)	−9.90	0.16
$Ar^+ + C_2H^+ + H$ (12)	−11.17	0.33
$Ar^+ + C_2H_2^+$ (13)	−16.23	0.02
Chemical reaction		
$ArC^+ + H^+ + C + H$ (14)	−2.50	0.001
$ArC^+ + C^+ + H + H$ (15)	−4.83	0.002
$ArC^+ + CH^+ + H$ (16)	−8.96	0.006

The table also lists $\Delta_r H^\circ$ [73], the literature value for the enthalpy of reaction. The branching ratios between the different channels measured at E_{cm} = 4.73 eV are also given. The branching ratios are directly derived from the number of counts in the peaks corresponding to the different reactive channels in the PSCO spectrum.

The sixteen channels arise from the general DET, SET and chemical reaction mechanisms discussed above and we will now consider each group of reactions in turn.

3.1. Double-electron-transfer reactions

Following collisions between Ar^{2+} and C_2H_2, we observe six reaction channels where the ion pair does not involve an Ar^+ monocation. These six channels clearly arise from DET processes, that is fragmentation of $C_2H_2^{2+}$ formed *via* the transfer of two electrons from C_2H_2 to Ar^{2+}. Fig. 2 shows two examples of scattering diagrams for these DET processes. Fig. 2(b) clearly shows the isotropic distribution of the CH^+ and H^+ products from reaction (2) about the velocity of the precursor C_2H_2 molecule $w(C_2H_2)$, a velocity which we can derive from the known velocity of the incident Ar^{2+} ion in the laboratory frame. Fig. 2(a) shows a similar distribution of the $w(CH^+)$ vectors about $w(C_2H_2)$ for reaction (4); however, for this channel the dead-time of the detector and the identical mass of the products restricts the scattering angle for one ion to less than 70° and the other ion to more than 110° in the laboratory frame. Scattering diagrams for the other DET channels show similar isotropic scattering of the ionic products about $w(C_2H_2)$.

In principle there are three mechanisms by which a DET reaction can occur. Specifically, the two direct DET pathways discussed above, concerted and sequential, plus a possible DET pathway *via* a $[Ar–C_2H_2]^{2+}$ intermediate which involves a longer term association of the reactants. If such complexation was the dominant pathway, we would not expect the fragment scattering to be centred on $w(C_2H_2)$, which is what we observe experimentally (Fig. 2). The dissociation of a long-lived complex, where the lifetime of the complex is much greater than its rotational period, to give the ionic products would result in the scattering of the products to be centred about the CM [35]. The scattering we observe, where the ionic products are scattered about $w(C_2H_2)$, is exactly that expected for a direct reaction mechanism, where the pair of electrons are transferred to the dication at a significant interspecies separation with little short-range Ar^{2+}–C_2H_2 interaction. If short-lived collision complex was formed, the products would not be scattered isotropically about the CM as one would expect for a long-lived complex. However, the formation of a short-lived complex would still involve some momentum exchange between the reactants and, hence, the products would not be scattered about $w(C_2H_2)$ as we observe experimentally. Thus, the DET reaction mechanism seems clearly to involve direct and long-range electron-transfer.

Considering the direct DET mechanisms described above, and illustrated in Fig. 1, the concerted DET process can be envisaged as occurring at a curve crossing between the $Ar^{2+} + C_2H_2$ and the $Ar + C_2H_2^{2+}$ potentials [40,64]. For the collision system under study we calculate that for the curve crossing to lie within the reaction window the product and reactant asymptotes must have a separation of less than 1 eV. Conversely, the sequential DET process (Fig. 1) involves two separate curve crossings, and should allow a wider range of exothermicities for efficient DET than the concerted mechanism. Thus, determining ΔE_T for the different DET process, and hence the exothermicity of the primary DET process, should provide an insight into the DET mechanism.

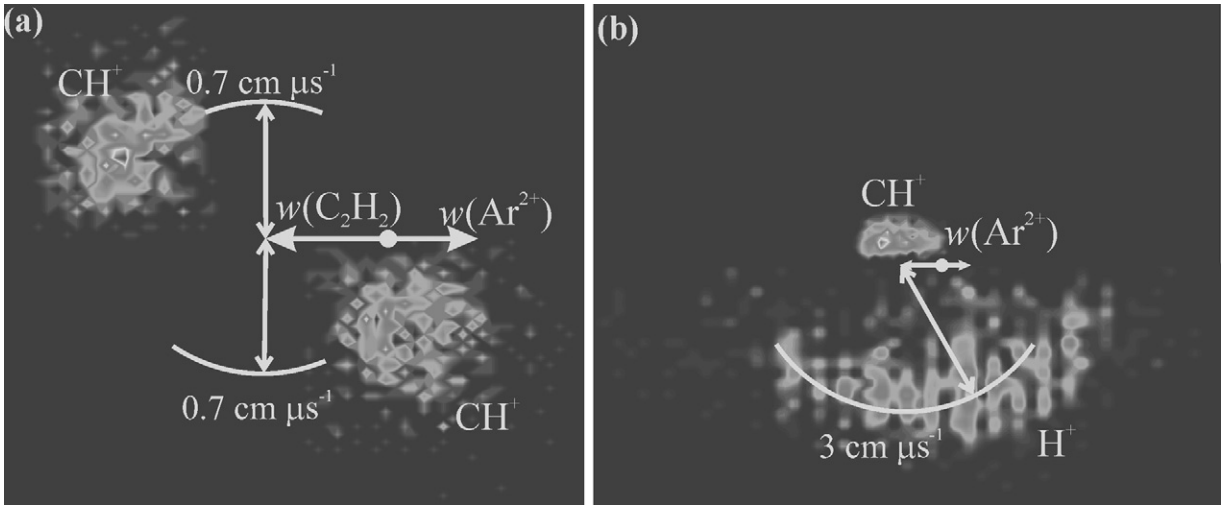

Fig. 2. CM scattering diagrams for the formation of (a) CH^+ and CH^+ and (b) CH^+ and H^+ following DET reactions of Ar^{2+} with C_2H_2 at a CM energy of 7.09 eV. In these diagrams the angular co-ordinate is the scattering angle θ between the reactant ion velocity and the velocity of the product [$0^\circ \le \theta \le 180^\circ$], and the radial co-ordinate is the magnitude of the CM velocity of the product. The CM is marked by the dot Data for one product is plotted in the upper half of the figure and for a second product in the lower half. In (a), due to deadtime losses at the detector, only the forward and backward scattered ions can be detected.

Table 2
Measured kinetic energy releases for the fragmentation of $C_2H_2^{2+}$ formed by DET to Ar^{2+}

Reaction	$C_2H_2^{2+}$ kinetic energy release (eV)[a]	$C_2H_2^{2+}$ precursor state energy (eV)	DET exothermicity (eV)	Kinetic energy release from photoionisation (eV) [22]
$C^+ + H^+ + CH + Ar$ (1)	5.7	43.4	0.0	5
$CH^+ + H^+ + C + Ar$ (2)	5.6	43.4	0.0	7
$CH^+ + C^+ + H + Ar$ (3)	7.0	42.4	1.0	5.7
$CH^+ + CH^+ + Ar$ (4)	7.2	38.5	4.9	5.4
$C_2^+ + H^+ + H + Ar$ (5)	6.5	42.4	1.0	6
$C_2H^+ + H^+ + Ar$ (6)	–	–	–	5.5

The corresponding $C_2H_2^{2+}$ precursor state energies are also shown and the derived exothermicity of the primary DET process (see text for details). The kinetic energy releases reported for the same fragmentation reactions induced by double photoionisation are also listed.

[a] Kinetic energy releases measured in this experiment. The KER values are an average of those measured for all five collision energies used in this study.

To determine the energy of the $C_2H_2^{2+}$ ions formed by the primary DET process, we can work in the frame of the reactant C_2H_2 molecules, as defined by $w(C_2H_2)$, and evaluate the kinetic energy released in the dissociation of the $C_2H_2^{2+}$ from the relative velocity vectors of the ionic fragmentation products. Table 2 lists the modal value of such kinetic energy distributions for the different DET channels. As expected, these kinetic energy distributions do not vary significantly with varying collision energy. Table 2 shows that the kinetic energy releases we determine for the different DET channels are broadly comparable to those for the same dissociation processes observed when $C_2H_2^{2+}$ is formed by photoionisation at 48 eV [22]. However, the relative intensities of the DET channels we observe differ markedly from those reported from photoionisation experiments. Where double ionisation of C_2H_2 occurs *via* DET, in our experiments, the formation of $CH^+ + C^+ + H$ (reaction (3)) is the major fragmentation channel. The fragmentations of $C_2H_2^{2+}$ to form $CH^+ + CH^+$, $C_2^+ + H^+ + H$ and $CH^+ + H^+$ are each approximately half as intense as reaction (3), whilst the formation of $C_2H^+ + H^+$ is weak. These branching ratios for the dissociation of $C_2H_2^{2+}$ are in contrast to those for the dication formed *via* photoionisation at 48 eV, where the dominant dissociation channel is $C_2H^+ + H^+$, followed by $CH^+ + CH^+$ formation and the production of $C_2^+ + H^+ + H$ [22].

The explanation for the different fragmentation patterns observed for $C_2H_2^{2+}$ formed by DET and by photoionisation is readily apparent if we estimate the precursor state energies (Table 2) for the $C_2H_2^{2+}$ electronic states that are formed in the primary DET process; the states which dissociate to yield the observed monocation pairs. Such state energies are estimated by adding the modal kinetic energy release we measure for the fragmentation of $C_2H_2^{2+}$ to the energy of the dissociation asymptote, expressed relative to the ground state of C_2H_2. It is important to note that such precursor state energies place a lower limit on the energy of the $C_2H_2^{2+}$ state which dissociated to give a particular ion pair, as they assume the fragmentation products are in their ground states. Such precursor state energies are listed in Table 2 and clearly show that, apart from reaction (4), the DET process are populating $C_2H_2^{2+}$ states lying approximately 42–44 eV above the ground sate of C_2H_2. In contrast, the non-resonant photoionisation experiments discussed above populate a range of dication states, which may be at markedly lower energies than the photon energy [22]. In particular, the photoionisation experiments populate lower lying states of $C_2H_2^{2+}$, which favour the dissociation to $CH^+ + CH^+$, $C_2H^+ + H^+$ and $CH_2^+ + C$. In fact, theoretical investigations indicate that the dominant source of the $CH_2^+ + H^+$ channel is the $^1\Delta_g$ state of $C_2H_2^{2+}$ at 32 eV from which ethyne can rearrange to the vinylidene structure [65]. This lower energy state is clearly not populated in DET between Ar^{2+} and C_2H_2. The precursor state for formation of $CH^+ + CH^+$ (4) in the DET reactions (Table 2) appears to lie at approximately 38 eV, markedly lower than the other precursor state energies we determine. Of course, this estimate of the precursor energy for reaction (4) assumes that the CH^+ products are formed in their ground states, but does agree well with an electronic state at 37 eV implicated in the formation CH^+ and CH^+ *via* photoionisation [22]. However, it is also possible that reaction (4) results from $C_2H_2^{2+}$ precursor state(s) at a similar energy (42–44 eV) to the other DET channels, but this precursor state dissociates to form vibronically excited CH^+ ions.

We can now determine the overall exothermicity of the primary DET process for each DET channel (given in Table 2) as the difference between precursor state energies of the primary $C_2H_2^{2+}$ species and the double ionisation potential of Ar. The small primary DET exothermicities we determine for all the channels, except reaction (4), are consistent with a concerted DET process (Fig. 1a). Indeed, the concerted picture of the DET process has been used to rationalize such reactions for highly charged ions [51]. The larger DET exothermicity we observe for the formation of CH^+ with CH^+, where the difference in energy between the $C_2H_2^{2+}$ precursor state PEC and the reactant PEC is around 5 eV, could indicate a sequential DET mechanism is operating for this reaction. However, as described above, a concerted mechanism populating a $C_2H_2^{2+}$ precursor state at 42–44 eV which dissociates to form excited CH^+ ions is also possible and, given the primary exothermicities observed for the other DET channels, perhaps more likely.

3.2. Single-electron-transfer reactions

There are seven channels (Table 1) in the PSCO spectrum (7)–(13) which can be attributed to transfer of a single electron from C_2H_2 to Ar^{2+}; six of these channels correspond to dissociative SET (7)–(12) together with a non-dissociative channel (13). For several of the dissociative SET channels there may be more than one neutral fragment formed along with the detected ions. For example, for production of the Ar^+ and CH^+ ion pairs (9) the accompanying neutral(s) could be CH or C and H. By comparing the translational exothermicity, derived from the PSCO spectrum, with the literature exothermicities it is often possible to deduce which neutral(s) are formed in such channels. In the example above, the literature enthalpy of reaction is calculated to be −7.0 eV if CH is the neutral or −3.5 eV if C and H are formed. The observed average translational exothermicity is approximately 6 eV, indicating that for this channel the neutral formed is CH. Similar arguments can be used to deduce neutral products for all the other SET reactions listed in Table 2. In all cases the assigned neutral products are strongly favoured by the TES derived from the PSCO spectrum.

The scattering diagrams derived from the PSCO data for the non-dissociative SET reaction (13) show strong forward scattering, as has been observed before for such processes [35,40,54,55,66]. That is, the Ar^+ product has a velocity which is predominantly directed in the same direction as $w(Ar^{2+})$. Similarly, $w(C_2H_2^+)$ is strongly aligned with the direction of $w(C_2H_2)$. Such scattering is consistent with the standard mechanism of such dication electron-transfer processes, where the reaction is direct and the electron

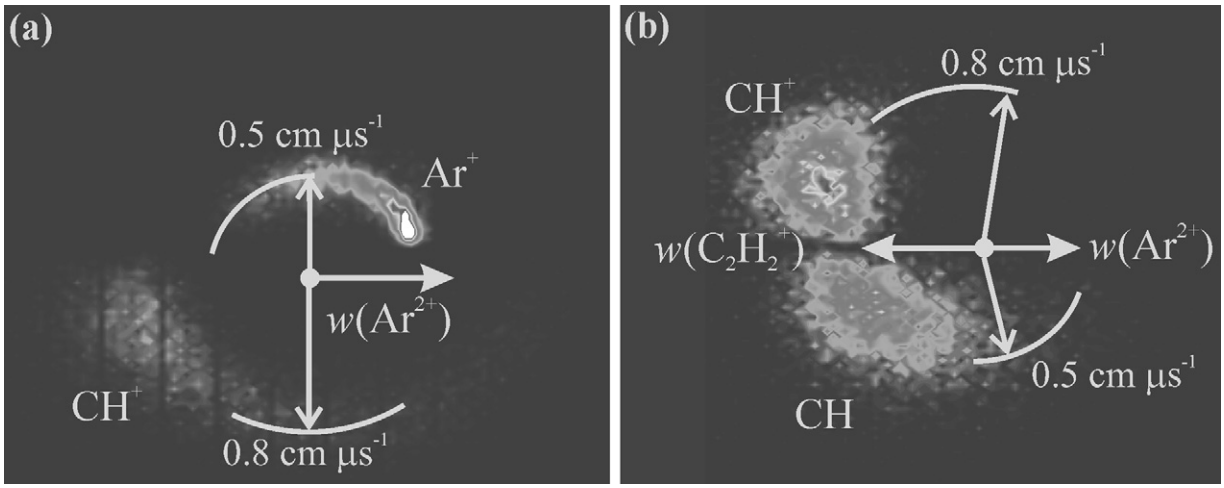

Fig. 3. CM and internal frame scattering diagrams for Ar^+, CH^+ and CH formed *via* SET at a CM energy of 7.09 eV. (a) A CM scattering diagram, see caption to Fig. 2 for details. (b) The internal frame scattering for CH^+ and CH with respect to the velocity of Ar^+. In (b) the angular co-ordinate is the scattering angle ϕ between the velocity of one product and the velocity of Ar^+ [$0^\circ \leq \phi \leq 180^\circ$], and the radial co-ordinate is the magnitude of the CM velocity of the product. Data for CH^+ relative to Ar^+ is plotted in the upper half of the figure and for CH relative to Ar^+ in the lower half.

is transferred at significant interspecies separations, although electron-transfer at short range has also been observed before [59].

All six dissociative SET channels exhibit very similar scattering diagrams and representative examples, for reaction (9), which generates $Ar^+ + CH^+ + CH$, are shown in Fig. 3. Fig. 3(a) shows that the Ar^+ product is again strongly forward scattered in the CM frame, whilst the CH^+ is scattered in the opposite direction, in the direction of $w(C_2H_2)$. Such strong forward scattering has also been observed before for dissociative SET processes, and is consistent with rapid direct transfer of an electron to Ar^{2+} from $C_2H_2^+$ at a significant interspecies separation (3–6 Å), forming an excited monocation which goes on to dissociate when well separated from the other ionic product [35,55,66].

One notable feature of the internal frame scattering diagrams for the dissociative SET channels (Fig. 3(b)) is that the velocities of the neutral species and monocation formed from the dissociation of the excited ethyne monocation ($C_2H_2^{+*}$) are not uniformly distributed about the same point in the scattering diagram. If the $C_2H_2^{+*}$ ion were to dissociate when effectively separate from the Ar^+ ion, the velocity vectors of the dissociation products would be isotropically distributed about $w(C_2H_2^{+*})$, as has been observed before for analogous reactions [35,55]. The expected velocity of the primary $C_2H_2^{+*}$ ion, $w(C_2H_2^{+*})$, can be determined by conservation of momentum from the known value of $w(Ar^+)$ and is marked in Fig. 3(b). We observe a distinct asymmetry in the distributions of the ionic and neutral products about $w(C_2H_2^{+*})$. The dissociation of the $C_2H_2^{+*}$ ion close to the Ar^+ ion, where the mutual electrostatic repulsion is significant, readily accounts for this observed asymmetry in the distribution of the products about $w(C_2H_2^{+*})$. In this situation, the ionic fragment receives an extra impulse due to the Coulombic repulsion from the Ar^+ ion, whilst the neutral fragment does not. Using a simple electrostatic model for the repulsion between Ar^+ and $C_2H_2^+$ it is possible to predict the approximate separation between Ar^+ and $C_2H_2^{+*}$ at which the hydrocarbon ion must dissociate to obtain the measured fragment velocities. This model indicates that the dissociation of $C_2H_2^{+*}$ must take place rapidly, within 500 fs, and within approximately 20 Å of the Ar^+ ion.

The ionisation energy of C_2H_2 is 11.40 eV[9] and the ionisation energy of Ar^+ is 27.63 eV. These ionisation energies result in approximately 16 eV of excess energy to distribute between product translation and the internal energy of the nascent $C_2H_2^+$ product following SET, if the Ar^{2+} and Ar^+ species are in their ground electronic states, as is shown below. In fact, from the average Ar^+ velocity for the dissociative SET channels we can deduce, by conservation of momentum, that approximately 4 eV of energy is deposited into the translation of the $C_2H_2^{+*}$ ion, still leaving approximately 12 eV as internal energy. This significant internal excitation of the nascent $C_2H_2^{+*}$ product explains the dominance of dissociative SET in the Ar^{2+}/C_2H_2 collision system (Table 2). The extent of dissociative SET from $Ar^{2+} + C_2H_2$ is in dramatic contrast with that observed in the complimentary reaction between $C_2H_2^{2+}$ and Ar; here, the SET reaction is exothermic by only approximately 4 eV and the product $C_2H_2^{+*}$ ion can have little internal energy and so non-dissociative SET dominates [60].

As with the fragmentation of $C_2H_2^{2+}$ formed by DET, we can compare the observed fragmentation patterns for the $C_2H_2^{+*}$ ions formed by SET with the fragmentation of this ion when formed by photoionisation. However, care must be taken in this comparison as in the SET reaction we are observing the decay of $C_2H_2^+$ ions formed with, on average, approximately 12 eV of internal energy. In contrast, $C_2H_2^+$ ions formed in non-resonant photoionisation experiments, where the photoelectron can carry away significant amounts of energy, are not constrained to such a specific internal energy content [9,10]. The appropriate comparison for the fragmentation of $C_2H_2^{+*}$ formed in the SET process is with $C_2H_2^+$ ions formed with known and comparable internal energies [16–20]. Such studies show that if the $C_2H_2^{+*}$ has enough internal energy to dissociate to $C_2H^+ + H^+$, long-lived $C_2H_2^+$ products are hardly observed [17,20]. Thus, the photoionisation results indicate that if $C_2H_2^{+*}$ is formed in the SET process with 12 eV of internal excitation, no long-lived $C_2H_2^+$ ions should be detected. However, we still clearly observe long-lived $C_2H_2^+$ ions from non-dissociative SET reactions (13), with a branching ratio of approximately 0.025 (Table 2). A ready explanation for our observation of these long-lived $C_2H_2^+$ ions is the presence of excited Ar^{2+} states, from the $3p^{-2}$ configuration, in the reactant dication beam. The reaction of $Ar^{2+}(^1D_2)$ with ethyne is sufficiently exothermic to form the ground electronic state of $C_2H_2^+$ together with the first excited state of $Ar^+(^2S)$. This non-dissociative SET reaction has a literature enthalpy of −4.5 eV, a value in excellent agreement with the translational exothermicity we observe for this channel; an exothermicity which places this reaction in the favoured "reaction window" for electron-transfer. Thus, is seems clear that the long-lived $C_2H_2^+$ ions we

observe arise from SET reactions of excited states of Ar^{2+}. Conversely, the experimentally determined exothermicities for the dissociative channels, channels which dominate the SET reactivity (Table 1), show that they are reactions of C_2H_2 with Ar^{2+} in its ^3P ground state and that the Ar^+ products formed are not electronically excited.

Unfortunately, no studies of the dissociation of energy-selected $C_2H_2^{+*}$ ions have been performed for ions with a comparable (12 eV) internal energy to the $C_2H_2^{+*}$ ions formed by the SET reactions. Energy-selected studies of photoionisation of C_2H_2 at 21 eV, where the $C_2H_2^+$ ion is formed with 9.6 eV of internal energy, observe just C_2H^+ as the final ionic product [17]. As expected, due to their larger internal energy content, the $C_2H_2^{+*}$ ions generated by SET between Ar^{2+} and C_2H_2 exhibit significantly more extensive fragmentation (Table 1) than $C_2H_2^{+*}$ ions formed with 9.6 eV internal energy. The major products of the dissociative SET reactions are C_2H^+, CH^+ and C_2^+, with H^+, C^+ and CH_2^+ also detected. The branching ratios between these different dissociative SET channels vary little with collision energy over the range (3–7 eV) investigated; the relative insensitivity of the cross-sections of SET reactions to the collision energy in this energy regime has been noted before [67].

Previously the SET reactions of Ar^{2+} and C_2H_2 have been investigated from near-thermal energies to 1 eV in a drift tube [33,34]. These drift tube experiments found that the reaction was rapid but saw only $C_2H_2^+$ and C_2H^+ as products, with $C_2H_2^+$ being the major product. The obvious reason for the difference between the PSCO experiment, where extreme fragmentation of $C_2H_2^{+*}$ is seen, and the drift tube results is the high buffer–gas pressures employed in the latter technique. These high pressures can lead to collisional stabilisation of any internally excited product ions.

A second estimate of the internal energy of the precursor $C_2H_2^{+*}$ products from dissociative SET can be made by addition of the measured ΔE_T values for the different channels to the energy of the appropriate dissociation asymptote. This estimate places a lower limit on the internal energy of the $C_2H_2^{+*}$ ion, as it assumes all the products are formed without any internal excitation. For all the observed dissociative SET channels, the above approach derives precursor $C_2H_2^{+*}$ states lying 12–15 eV above the energy of ground state $C_2H_2^+$, 23.5–26.5 eV above the ground state of C_2H_2. Satisfyingly, this range of precursor state energies is consistent with our initial estimate of the internal excitation of the $C_2H_2^{+*}$ ion made above, *via* conservation of momentum. The $C^2\Sigma_g^+$ state of $C_2H_2^+$ lies approximately 24 eV above the ground state of C_2H_2, in precisely this energy regime, together with a manifold of quartet electronic states which have been the focus of recent interest [68]. The dissociation of the $C^2\Sigma_g^+$ state, and higher lying doublet states, is thought to play a major role in the fragmentation of $C_2H_2^+$ ions with internal energies similar to the primary products of the SET reactions we have identified above. The predissociation of these doublet states by the quartet states has also been investigated [68–70], and seems to contribute significantly to the yield of CH^+ dissociation products [70]. Thus, the increased propensity for the $C_2H_2^{+*}$ ions formed by SET to dissociate to yield CH^+, in comparison with $C_2H_2^{+*}$ ions with a lower internal energy content, is consistent with the known behaviour of the electronic states of $C_2H_2^+$ lying 12–15 eV above the ionic ground state.

3.3. Chemical reactions

Following collisions of Ar^{2+} with C_2H_2, three channels involving the formation of ArC^+ are detected (14)–(16). Indeed, the formation of new chemical bonds involving rare gas atoms, following the collisions between dications and neutral molecules, has been observed before [71,72]. Previous studies of the dynamics of bond-forming reactions of molecular dications have shown that most, but not all, of these bond-forming processes proceed *via* complexation [35,42]. The scattering diagrams for the chemical channels forming ArC^+ (Fig. 4) are, surprisingly, very similar to the scattering diagrams for the SET reactions. Specifically, in the CM frame the ArC^+ product is forward scattered, in the direction of the original Ar^{2+} velocity, whilst the second ionic product (H^+ or C^+ or CH^+) is scattered in the opposite direction. This scattering indicates that the reaction is effectively direct, involving little or no complexation. A mechanism consistent with the observed scattering is one in which Ar^{2+} strips a CH^- group from C_2H_2 to form $ArCH^{+*}$ and CH^+. The $ArCH^{+*}$ subsequently dissociates to ArC^+ which we observe in coincidence with CH^+ (channel 16) or the products of the dissociation of the CH^+ ion (H^+, C^+, channels 14 and 15). This proposed mechanism is supported by the internal frame scattering of CH^+ and H relative to $w(ArC^+)$ for reaction (16) (Fig. 4). This internal frame scattering diagram shows that the velocity of CH^+ is strongly anti-correlated with that of ArC^+, and the velocity of the H atom is broadly correlated with that of ArC^+. This scattering is consistent with the initial separation of $ArCH^+$ and CH^+ and the subsequent dissociation of $ArCH^+$.

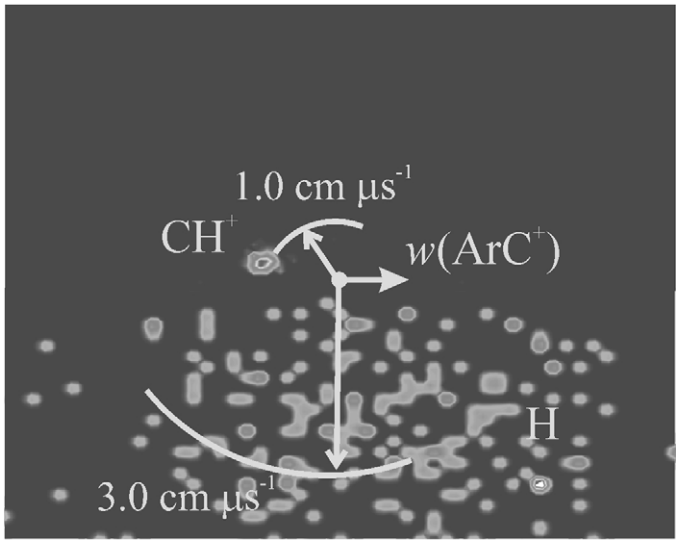

Fig. 4. Internal frame scattering diagram for CH^+ and H relative to the velocity of ArC^+ for the chemical reaction (16) following collisions of Ar^{2+} with C_2H_2 at a CM energy of 4.73 eV.

Another possible mechanism for the formation of ArC^+ is that the Ar^{2+} abstracts a carbon anion from C_2H_2 to form ArC^+ and CH_2^+. Such a mechanism might be possible if the presence of the Ar^{2+} induces isomerisation of the ethyne to a vinylidene structure. Such an isomerisation would perhaps be expected to proceed *via* a long-lived complex. Indeed, calculations of the $C_2H_2^{2+}$ + Ar potential energy surface [60] show a route to formation of ArC^+ with CH_2^+, which involves the formation of a complex. However, the clear signature of a direct reaction mechanism given by the observed experimental scattering (Fig. 4) and the correlation of the velocity of the neutral species with the ArC^+ product strongly indicates that the formation of ArC^+ proceeds *via* initial formation of $ArCH^+$, and not by transfer of a carbon anion.

There is no experimental enthalpy of formation for ArC^+ available. Using existing thermochemistry, and given that the measured experimental translational exothermicity for channel (16) is ~9 eV, we derive an upper limit for ΔH_f [ArC^+] of 17.7 eV. This value is in excellent agreement with that of Lu et al., a value based on previous theoretical studies and thermochemistry [71].

As the collision energy is increased, the branching ratio for forming $ArC^+ + CH^+$ (16) appears to decrease significantly. Such a decrease, without a comparable increase in the branching ratios for reactions (14) and (15), is readily explained by increased fragmentation of the ArC^+ ion due to its formation with increasing internal energy content as the collision energy increases.

It is interesting to note that ArC^+ is the only chemical product detected from the reaction of Ar^{2+} with C_2H_2 and this chemical channel does not have a large branching ratio. In contrast, ArH^+ formation is a major channel following the reaction of $C_2H_2{}^{2+}$ with Ar [60]. This difference in reactivity is easily explicable as $C_2H_2{}^{2+}$ can readily act as a proton donor, but extraction of a hydride ion by Ar^{2+} from C_2H_2 to form ArH^+ is not expected to be a facile process.

4. Conclusions

The reactions of Ar^{2+} with C_2H_2 which produce pairs of monocations have been studied using a coincidence technique at centre-of-mass collision energies ranging from 3 to 7 eV. Nine different monocationic products were detected, involved in sixteen separate reaction channels. Three general classes of reactivity were observed: DET, SET and bond-forming chemical reactions.

Careful examination of the scattering diagrams and energetics extracted from the coincidence data indicate that DET reaction is direct and the energetics hint at concerted two-electron-transfer. As is commonly observed, SET from C_2H_2 to Ar^{2+} takes place *via* a direct mechanism and does not involve complexation. Most of the $C_2H_2{}^+$ products that are formed in the SET reactions possess significant (12–15 eV) internal energy and fragment rapidly within the electric field of the partner Ar^+ ion. The chemical reactions, which form ArC+, proceed *via* a direct mechanism involving the initial formation of an $ArCH^+$ ion, which subsequently fragments to form ArC^+.

Acknowledgements

These experiments have received the support of the EPSRC. JFL thanks the EPSRC for the award of a research studentship. We are particularly grateful to Zdenek Herman for his long-standing interest in dicationic reactivity and for many illuminating discussions on ionic reactions, and opera, in Prague, London and at many SASP conferences.

References

[1] M. Herman, Mol. Phys. 105 (2007) 2217.
[2] B.J. Orr, Int. Rev. Phys. Chem. 25 (2006) 655.
[3] I.A. Larionova, B.S. Fialkov, K.Y. Kalinich, A.B. Fialkov, B.S. Ospanov, Combust. Explos. Shock Waves 29 (1993) 341.
[4] F.J. Gordillo-Vázquez, J.M. Albella, Plasma Sources Sci. Technol. 11 (2002) 498.
[5] M.C. McMaster, W.L. Hsu, M.E. Coltrin, D.S. Dandy, C. Fox, Diamond Relat. Mater. 4 (1995) 1000.
[6] L. Marcinauskasa, A. Grigonis, V. Kulikauskas, V. Valincius, Vacuum 81 (2007) 1220.
[7] R. Courtin, D. Gautier, A. Marten, B. Bezard, R. Hanel, Astrophys. J. 287 (1984) 899.
[8] M.J. McEwan, G.B.I. Scott, V.G. Anicich, Int. J. Mass Spectrom. Ion Proc. 172 (1998) 209.
[9] R.A. Mackie, S.W.J. Scully, A.M. Sands, R. Browning, K.F. Dunn, C.J. Latimer, Int. J. Mass Spectrom. 223/224 (2003) 67.
[10] T. Hayaishi, S. Iwata, M. Sasanuma, E. Ishiguro, Y. Morioka, Y. Iida, M. Nakamura, J. Phys. B 15 (1982) 79.
[11] J. Berkowitz, Photoabsorption, Photoionization and Photoelectron Spectroscopy, Academic Press, New York, 1979.
[12] R. Botter, V.H. Dibeler, J.A. Walker, H.M. Rosenstock, J. Chem. Phys. 44 (1966) 1271.
[13] D.M.P. Holland, M.A. MacDonald, M.A. Hayes, L. Karlsson, B. Wannberg, J. Electron. Spectrosc. Relat. Phenom. 104 (1999) 245.
[14] L. Avaldi, G. Dawber, R.I. Hall, G.C. King, A.G. McConkey, M.A. MacDonald, G. Stefani, J. Electron. Spectrosc. Relat. Phenom. 71 (1995) 93.
[15] J.E. Reutt, L.S. Wang, J.E. Pollard, D.J. Trevor, Y.T. Lee, D.A. Shirley, J. Chem. Phys. 84 (1986) 3022.
[16] G.K. Jarvis, K.-M. Weitzel, M. Malow, T. Baer, Y. Song, C.Y. Ng, Phys. Chem. Chem. Phys. 1 (1999) 5259.
[17] C. Servais, R. Locht, Chem. Phys. Lett. 236 (1995) 96.
[18] K.-M. Weitzel, J. Mähnert, M. Penno, Chem. Phys. 187 (1994) 117.
[19] K.-M. Weitzel, J. Mähnert, M. Penno, Chem. Phys. Lett. 224 (1994) 371.
[20] J.H.D. Eland, Int. J. Mass Spectrom. Ion Phys. 31 (1979) 161.
[21] S.J. King, S.D. Price, J. Chem. Phys. 127 (2007) 174307.
[22] R. Thissen, J. Delwiche, J.M. Robbe, D. Duflot, J.P. Flament, J.H.D. Eland, J. Chem. Phys. 99 (1993) 6590.
[23] J.H.D. Eland, F.S. Wort, P. Lablanquie, I. Nenner, Z. Phys. D 4 (1986) 31.
[24] R.I. Hall, L. Avaldi, G. Dawber, A.G. McConkey, M.A. Macdonald, G.C. King, Chem. Phys. 187 (1994) 125.
[25] N. Jeffreys, S.R. Andrews, D.E. Parry, F.M. Harris, Rapid Commun. Mass Spectrom. 10 (1996) 1693.
[26] O. Furuhashi, T. Kinugawa, S. Masuda, C. Yamada, S. Ohtani, Chem. Phys. Lett. 342 (2001) 625.
[27] S. De, J. Rajput, A. Roy, P.N. Ghosh, C.P. Safvan, Phys. Rev. A 77 (2008) 022708.
[28] R.R. Rye, T.E. Madley, J.E. Houston, P.H. Holloway, J. Chem. Phys. 69 (1978) 1504.
[29] M. Thompson, P.A. Hewitt, D.S. Wooliscroft, Anal. Chem. 48 (1976) 1336.
[30] T. Osipov, T.N. Rescigno, T. Weber, S. Miyabe, T. Jahnke, A.S. Alnaser, M.P. Hertlein, O. Jagutzki, L. Ph, H. Schmidt, M. Schöffler, L. Foucar, S. Schössler, T. Havermeier, M. Odenweller, S. Voss, B. Feinberg, A.L. Landers, M.H. Prior, R. Dörner, C.L. Cocke, A. Belkacem, J. Phys. B 41 (2008) 091001.
[31] J. Roithová, D. Schröder, J. Am. Chem. Soc. 128 (2006) 4208.
[32] S. Petrie, G. Javahery, J. Wang, D.K. Bohme, J. Phys. Chem. 96 (1992) 6121.
[33] H. Störi, E. Alge, H. Villinger, F. Egger, W. Lindinger, Int. J. Mass Spectrom. Ion Phys. 30 (1979) 263.
[34] W. Lindinger, E. Alge, H. Störi, M. Pahl, R.N. Varney, J. Chem. Phys. 67 (1977) 3495.
[35] S.D. Price, Int. J. Mass Spectrom. 260 (2007) 1.
[36] S.D. Price, Phys. Chem. Chem. Phys. 5 (2003) 1717.
[37] N. Tafadar, D. Kearney, S.D. Price, J. Chem. Phys. 115 (2001) 8819.
[38] S.D. Price, M. Manning, S.R. Leone, J. Am. Chem. Soc. 116 (1994) 8673.
[39] S.D. Price, M. Manning, S.R. Leone, Chem. Phys. Lett. 214 (1993) 553.
[40] Z. Herman, Int. Rev. Phys. Chem. 15 (1996) 299.
[41] D. Schroder, H. Schwarz, J. Phys. Chem. A 103 (1999) 7385.
[42] J. Roithova, C.L. Ricketts, D. Schroder, S.D. Price, Angew. Chem. Int. Ed. 46 (2007) 9316.
[43] J. Roithová, D. Schröder, Phys. Chem. Chem. Phys. 9 (2007) 731.
[44] S.A. Rogers, S.D. Price, S.R. Leone, J. Chem. Phys. 98 (1993) 280.
[45] P.W. Burnside, S.D. Price, Phys. Chem. Chem. Phys. 9 (2007) 3902.
[46] J.S. Miller, S.H. Pullins, D.J. Levandier, Y. Chiu, R.A. Dressler, J. Appl. Phys. 91 (2002) 984.
[47] H. von Koding, N.M.M. Nibbering, Int. J. Mass Spectrom. 187 (1999) 281.
[48] R.H. Neynaber, S.Y. Tang, Chem. Phys. Lett. 92 (1982) 556.
[49] K. Okuno, T. Koizumi, Y. Kaneko, Phys. Rev. Lett. 40 (1978) 1708.
[50] O. Hadjar, D. Ascenzi, D. Bassi, P. Franceschi, M. Sabido, P. Tosi, Chem. Phys. Lett. 400 (2004) 476.
[51] T.P. Grozdanov, R.K. Janev, J. Phys. B: At. Mol. Opt. Phys. 13 (1980) 3431.
[52] D. Smith, N.G. Adams, E. Alge, H. Villinger, W. Lindinger, J. Phys. B: At. Mol. Opt. Phys. 13 (1980) 2787.
[53] W.-P. Hu, S.M. Harper, S.D. Price, Meas. Sci. Technol. 13 (2002) 1512.
[54] S.M. Harper, W.-P. Hu, S.D. Price, J. Phys. B 35 (2002) 4409.
[55] W.P. Hu, S.M. Harper, S.D. Price, Mol. Phys. 103 (2005) 1809.
[56] L. Wåhlin, Nucl. Instrum. Methods 27 (1964) 55.
[57] C.L. Ricketts, S.M. Harper, S.W.P. Hu, S.D. Price, J. Chem. Phys. 123 (2005) 134322/1.
[58] S.M. Harper, S.W.P. Hu, S.D. Price, J. Chem. Phys. 121 (2004) 3507.
[59] S.M. Harper, S.W.P. Hu, S.D. Price, J. Chem. Phys. 120 (2004) 7245.
[60] D. Ascenzi, P. Tosi, J. Roithová, C.L. Ricketts, D. Schröder, J.F. Lockyear, M.A. Parkes, S.D. Price, Phys. Chem. Chem. Phys., in press.
[61] B. Friedrich, Z. Herman, Chem. Phys. Lett. 104 (1984) 375.
[62] T. Nakamura, N. Kobayashi, Y. Kaneko, J. Phys. Soc. Jpn. 54 (1985) 2774.
[63] NIST Atomic Spectra Database Revision 3.1.5, Y. Ralchenko, A.E. Kramida, J. Reader, N.A. Team, National Institute of Standards and Technology, Gaithersburg, MD, 2008.
[64] S.D. Price, J. Chem. Soc., Faraday Trans. 93 (1997) 2451.
[65] T.S. Zyubina, Y.A. Dyakov, S.H. Lin, A.D. Bandrauk, A.M. Mebel, J. Chem. Phys. 123 (2005) 134320.
[66] L. Mrazek, J. Zabka, Z. Dolejsek, J. Hrusak, Z. Herman, J. Phys. Chem. A 104 (2000) 7294.
[67] C.L. Ricketts, D. Schröder, J. Roithova, H. Schwarz, R. Thissen, O. Dutuit, J. Žabka, Z. Herman, S.D. Price, Phys. Chem. Chem. Phys. 10 (2008) 5135–5143.
[68] M. Hochlaf, S. Taylor, J.H.D. Eland, J. Chem. Phys. 125 (2006) 214301.
[69] R. Locht, M. Davister, Chem. Phys. 195 (1995) 443.
[70] M. Davister, R. Locht, Chem. Phys. 191 (1995) 333.
[71] W. Lu, P. Tosi, D. Bassi, J. Chem. Phys. 112 (2000) 4648.
[72] P.W. Burnside, S.D. Price, Int. J. Mass Spectrom. 249/250 (2006) 279.
[73] P.J. Linstrom, W.G. Mallard (Eds.), NIST Chemistry WebBook, NIST Standard Reference Database Number 69, National Institute of Standards and Technology, Gaithersburg MD, June 2005 (http://webbook.nist.gov).